

See discussions, stats, and author profiles for this publication at: <https://www.researchgate.net/publication/231272513>

Atomic Force Microscopy (AFM) Investigation on the Surfactant Wettability Alteration Mechanism of Aged Mica Mineral Surfaces

ARTICLE in ENERGY & FUELS · DECEMBER 2010

Impact Factor: 2.79 · DOI: 10.1021/ef100699t

CITATIONS

29

READS

211

6 AUTHORS, INCLUDING:



Mohammad Hadi Ghatte

Shiraz University

71 PUBLICATIONS 744 CITATIONS

SEE PROFILE



Shahab Ayatollahi

Sharif University of Technology

197 PUBLICATIONS 1,169 CITATIONS

SEE PROFILE

Atomic Force Microscopy (AFM) Investigation on the Surfactant Wettability Alteration Mechanism of Aged Mica Mineral Surfaces

Omolbanin Seiedi,[†] Marziyeh Rahbar,[†] Moein Nabipour,^{*,‡} Mohammad A. Emadi,[§]
Mohammad H. Ghatte,^{||} and Shahab Ayatollahi[†]

[†]Enhanced Oil Recovery (EOR) Research Center, School of Chemical and Petroleum Engineering, Shiraz University, Post Office Box 71345-1719, Shiraz, Iran, [‡]Chemical Engineering Department, Islamic Azad University, Marvdasht Branch, Marvdasht, Iran, [§]Research and Technology Directorate, National Iranian Oil Company (NIOC), Tehran 1969813771, Iran, and ^{||}Department of Chemistry, College of Science, Shiraz University, Shiraz 71454, Iran

Received June 6, 2010. Revised Manuscript Received November 22, 2010

In this study, the mica samples aged in crude oil were treated by two types of surfactants: Triton X-100 and C₁₆TAB, to find the mechanisms of wettability alteration. The contact angle measurements were conducted stepwise to check the wettability alteration of the mica surfaces. Atomic force microscopy (AFM) topographies and phase images were obtained and used to investigate the effects of aging in crude oil and surfactant treatment of the mica surface. The results show that the solution of Triton X-100/brine changes the wettability of the mica surface aged in crude oil to water-wet; however, the solution of C₁₆TAB/brine alters the aged mica surface to more oil-wet conditions. Fractal measurement was used to check the AFM images for quantitative assessment of the surface roughness for wettability alteration investigation. Two different mechanisms proposed here are the surface cleaning and the surfactant adsorption for Triton X-100 and C₁₆TAB, respectively.

Introduction

Water-flooding as a secondary oil recovery process is shown to be effective for water-wet fractured reservoirs; however, large amounts of oil would remain in the oil-wet matrix after water-flooding. Wettability alteration of the oil-wet rocks to water-wet or intermediate-wet conditions is proposed as an effective mechanism to improve the oil recovery efficiency.^{1,2} Surfactant-based chemical flooding is a well-known process for residual oil recovery from the rock matrixes after water-flooding.^{3–8} The two main mechanisms proposed for surfactant injection are wettability alteration of the rock to allow for self-imbibition of water^{9–11} and

interfacial tension (IFT) reduction to ultra-low values.^{12,13} Thus, the imbibition improves oil recovery if very dilute surfactant solutions are used. Zhang et al.^{12,14} evaluated several ethoxylated and propoxylated sulfates in the presence of a low alkaline concentration. They have found that IFT of surfactant solutions was changed to ultra-low values ($\sim 10^{-3}$ mN/m).

Use of surfactants for wettability alteration of chalk and dolomite cores to enhance their potential for spontaneous imbibition has also been investigated.^{5–8,15,16} Standnes and Austad⁶ have examined the spontaneous imbibition of different surfactants into oil-wet chalk. They have shown that cationic surfactants alter the rock wettability to a more water-wet state by desorbing organic carboxylates from the rock surface. Chen et al.¹⁷ have checked the ability of non-ionic and anionic surfactants to alter the wetting characteristics of rocks toward less oil-wet. Strand et al.⁷ have also checked both non-ionic and cationic surfactants with a strategy to alter wettability but avoided ultra-low IFT. They have also used some surface-active chemicals to improve the spontaneous imbibition of water into oil-wet carbonates using

*To whom correspondence should be addressed. E-mail: nabipour@gmail.com.

(1) Seethepalli, A.; Adibhatla, B.; Mohanty, K. K. Wettability alteration during surfactant flooding of carbonate reservoirs. *Proceedings of the 14th Society of Petroleum Engineers (SPE) Department of Energy (DOE) Symposium on Improved Oil Recovery (IOR)*; Tulsa, OK, April 17–21, 2004; SPE 89423.

(2) Karabakal, U.; Bagci, S. *Energy Fuels* **2004**, *18*, 438–449.

(3) Nabipour, M.; Escrochi, M.; Ayatollahi, Sh.; Boukadi, F.; Wadhahi, M.; Maamari, R.; Bemani, R. *J. Pet. Sci. Eng.* **2006**, *55*, 74–82.

(4) Spinler, E. A.; Zornes, D. R.; Tobola, D. P.; Moradi-Araghi, A. Enhancement of oil recovery using low concentration surfactant to improve spontaneous or forced imbibition in chalk. *Proceedings of the Society of Petroleum Engineers (SPE) Department of Energy (DOE) Improved Oil Recovery Symposium*; Tulsa, OK, April 3–5, 2000; SPE 59290.

(5) Standnes, D. C.; Austad, T. *J. Pet. Sci. Eng.* **2000**, *28*, 111–121.

(6) Standnes, D. C.; Austad, T. *J. Pet. Sci. Eng.* **2000**, *28*, 123–143.

(7) Strand, S.; Standnes, D. C.; Austad, T. *Energy Fuels* **2003**, *17*, 1133–1144.

(8) Standnes, N. C.; Austad, T. *Colloids Surf., A* **2003**, *216*, 243–259.

(9) Standnes, D. C.; Nogaret, L. A. D.; Chen, H. L.; Austad, T. *Energy Fuels* **2002**, *16*, 1557–1564.

(10) Høgnesen, E. J.; Standnes, D. C.; Austad, T. *Energy Fuels* **2004**, *18*, 1665–1675.

(11) Fathi, S. J.; Austad, T.; Strand, S. *Energy Fuels* **2010**, *24*, 2514–2519.

(12) Hirasaki, G.; Zhang, D. L. Surface chemistry of oil recovery from fractured, oil-wet, carbonate formations. *Proceedings of the Society of Petroleum Engineers (SPE) International Symposium on Oil Field Chemistry*; Houston, TX, Feb 5–8, 2003; SPE 88365.

(13) Aoudia, M.; Al-Maamari, R. S.; Nabipour, M.; Al-Bemani, A. S.; Ayatollahi, Sh. *Energy Fuels* **2010**, *24*, 3655–3663.

(14) Zhang, D. L.; Liu, S.; Puerto, M.; Miller, C. A.; Hirasaki, G. J. *J. Pet. Sci. Eng.* **2006**, *52*, 213–226.

(15) Austad, T.; Milter, J. Spontaneous imbibition of water into low permeable chalk at different wettabilities using surfactants. *Proceedings of the Society of Petroleum Engineers (SPE) International Symposium on Oilfield Chemistry*; Houston, TX, Feb 18–21, 1997; SPE 37236.

(16) Austad, T.; Matre, B.; Milter, J.; Seavareid, A.; Oyno, L. *Colloids Surf., A* **1998**, *137*, 117–129.

(17) Chen, H. L.; Lucas, L. R.; Nogaret, L. A. D.; Yang, H. D.; Kenyan, D. E. *SPE Reservoir Eval. Eng.* **2001**, *4*, 16–25.

aqueous solutions of an ethoxylated alcohol (EA) and the cationic surfactant C₁₂TAB. Contact angle measurements on oil-wet calcite crystals have confirmed that C₁₂TAB is much more effective than EA in altering wettability toward more water-wet conditions by measuring the advancing contact angles on calcite surfaces.⁹ Ayirala et al.¹⁸ have studied the effect of a non-ionic surfactant (ethoxy alcohol) and an anionic surfactant (ethoxy sulfate). They have also used several anionic surfactants in the presence of sodium carbonate to change the wettability of the solid surfaces. Most of the used anionic surfactants could alter the wettability of calcite surfaces better than a cationic surfactant, such as dodecyltrimethylammonium bromide (DTAB).

Nanotechnology application can be found in different elements of oil production activities, for example, using surfactants for wettability alteration to increase the oil production from wellbores by removing oil-based mud residue.¹⁹ Atomic force microscopy (AFM) as a tool for the nano-scale study of the surfaces has been used recently as an effective means for wettability studies. Lord and Buckley²⁰ have used AFM to study the change of mica surface topography before and after aging in crude oil. They have examined the effect of aging time, position of the substrate, and crude oil composition on the surface topography. Basu and Sharma^{21–23} have used AFM to measure the forces between a coated AFM tip and a mineral surface in brine. They have found that the composition of the oil phase plays an important role in the stability of the brine films, because it is the main barrier for direct contact between the rock surface and crude oil.

The mechanism of wettability alteration by crude oil components and surfactants is important to establish efficient methods for chemical flooding. A limited number of publications can be found on this topic in the literature. In the two recent works, the mineral-treated surfaces have been monitored by AFM and the wettability of the mineral treated by crude oil components and surfactants studied by contact angle measurement. It has been shown that the anionic surfactants can remove the adsorbed components from the mineral surface and induce the wettability to preferential water-wet.^{24,25} Also, it is demonstrated that the adsorption/removal mechanism affects the wettability of the mica surface when polyethoxylated amines with different ethoxy groups and chain

| number | test name | test method | result (wt %) |
|--------|--------------------|-------------|---------------|
| 1 | saturate content | SARA test | 45 |
| 2 | aromatic content | SARA test | 32 |
| 3 | asphaltene content | SARA test | 5 |
| 4 | resin content | SARA test | 8 |

lengths are used as surfactants. AFM images have been shown to be qualitatively consistent with the interpretations of macroscopic contact angle measurements.²⁶

In this work, cationic and non-ionic surfactants are used to monitor the surface modification and the mechanisms of wettability alteration of the aged mica surface. AFM images are obtained, and the results are verified by comparing to the contact angle measurements. Topography images are used to confirm the deposition/removal of the components on the mica surfaces, before and after surfactant treatments. Surface fractal dimension as the quantitative assessment based on the statistical parameters from the images is applied to assess the surface roughness during each treatment.

Experimental Section

Substrate. The mica used for the AFM test was microscopically smooth enough for AFM imaging.²⁰ The peeled fresh mica was used as a raw solid surface for the aging and surfactant-treating processes.

Oil. The crude oil was provided from an oil field, located in the south of Iran, with 32° American Petroleum Institute (API), 18 cP viscosity at 25 °C, and acid number of 3.7 mg of KOH/g of sample. The crude oil compositions [saturates, aromatics, resins, and asphaltenes (SARA) fraction] are shown in Table 1.

Brine. Synthetic brine was prepared according to the Bangestan formation in Iran. The original formation salinity is about 200 000 ppm of solids. The pH and density (at 20 °C) for synthetic brine were found to be 5.5 and 1.1 g/cm³, respectively. More information regarding the brine and oil composition can be found elsewhere.²⁷

Chemicals. The properties of the surfactants are given in Table 2. The cationic surfactant (C₁₆TAB) and the non-ionic surfactant (Triton X-100) were purchased from the Merck Company.

Sample Preparation. Peeled mica was gently immersed in brine (0.1 M NaCl) for 16 h at room temperature (23 °C). The soaked samples were then removed from the aqueous solution and immediately soaked in the crude oil for 3 days at 80 °C. The samples were then soaked in surfactant/brine solutions for 2 days at room temperature. Then, the samples were washed with distilled water.^{20,24}

Topography and Phase Images. Three mica plates were used for the tests performed in this study. All of the plates were soaked in the brine simultaneously and then aged in crude oil (known as aged mica in this study). One of these aged-mica plates was used as a blank. One was placed in C₁₆TAB solution. The last one was placed in Triton X-100 solution. All of the plates were finally rinsed with water and dried in air before taking the AFM pictures. Surfaces were monitored using Dual-Scope DS 95 AFM and DME image software. All experiments were performed at room temperature by scanning the surfaces with a silicon tip in non-contact mode.

(26) Bryant, E. M.; Bowman, R. S.; Buckley, J. S. *J. Pet. Sci. Eng.* **2006**, 52, 244–252.

(27) Seiedi, O.; Nabipour, M.; Mogharebian, S.; Bahar, N.; Ayatollahi, Sh.; Ghatee, M. H. Macroscopic, microscopic investigation of wettability alteration of Iranian oil field rock using surfactants. *Proceedings of the 10th International Symposium on Reservoir Wettability*; Abu Dhabi, United Arab Emirates, Oct 26–28, 2008.

(18) Ayirala, S. C.; Vijapurapu, C. S.; Rao, D. N. *J. Pet. Sci. Eng.* **2006**, 52, 261–274.

(19) Zanten, R. V.; Ezzat, D. Surfactant nanotechnology offers new method for removing oil-based mud residue to achieve fast, effective wellbore cleaning and remediation. *Proceedings of the Society of Petroleum Engineers (SPE) International Symposium and Exhibition on Formation Damage Control*; Lafayette, LA, Feb 10–20, 2010; SPE 127884.

(20) Lord, D. L.; Buckley, J. S. *Colloids Surf., A* **2002**, 206, 531–546.

(21) Basu, S.; Sharma, M. M. Characterization of mixed wettability states in oil reservoirs by atomic force microscopy. *Proceedings of the Society of Petroleum Engineers (SPE) Annual Technical Conference and Exhibition*; Denver, CO, Oct 22–25, 1996; SPE 35572.

(22) Basu, S.; Sharma, M. M. *J. Colloid Interface Sci.* **1996**, 181, 443–455.

(23) Basu, S.; Sharma, M. M. Investigating the role of crude-oil components on wettability alteration using atomic force microscopy. *Proceedings of the Society of Petroleum Engineers (SPE) International Symposium on Oilfield Chemistry*; Houston, TX, Feb 18–21, 1997; SPE 37231.

(24) Kumar, K.; Dao, E. K.; Mohanty, K. K. Atomic force microscopy study of wettability alteration by surfactants. *Proceedings of the Society of Petroleum Engineers (SPE) International Symposium on Oilfield Chemistry*; Houston, TX, Feb 2–5, 2005; SPE 93009.

(25) Kumar, K.; Dao, E. K.; Mohanty, K. K. *J. Colloid Interface Sci.* **2005**, 289, 206–217.

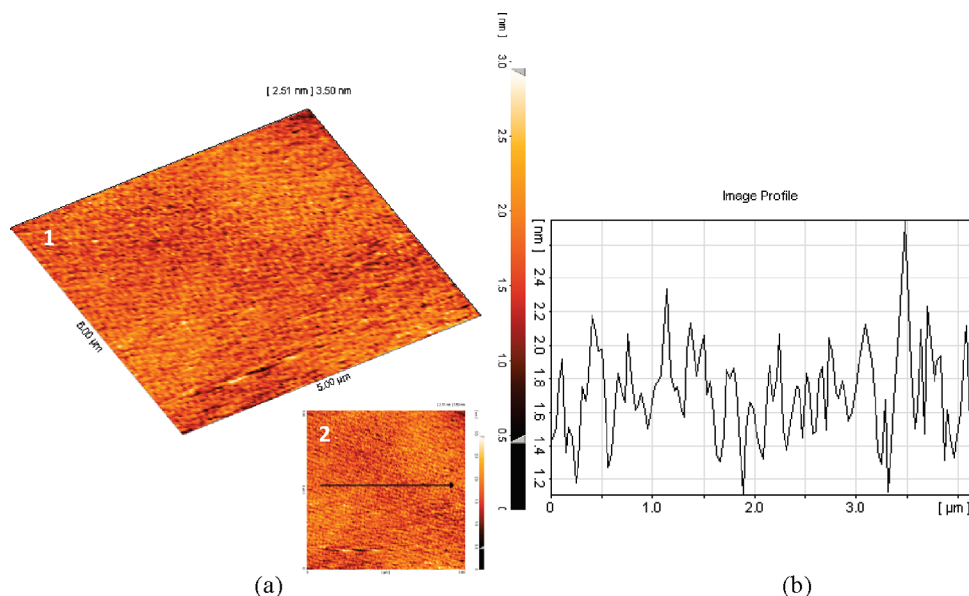


Figure 1. Fresh mica surfaces scanned by AFM: (a-1) height image, (a-2) height image with a selected path, and (b) surface profile based on the chosen path.

Table 2. Surfactant Property

| Surfactant | type | Molecular Structure | Chemical formulation | Concentration (wt.%) | IFT (dyn/cm) | CMC (wt.%) |
|---------------------|-----------|---------------------|--|-------------------------|-----------------|---------------|
| C ₁₆ TAB | Cationic | | n-C ₁₆ -N-(CH ₃) ₃ -Br | 1 | 0.9 | 0.03 |
| TritonX-100 | Non-ionic | | C ₁₄ H ₂₂ O(C ₂ H ₄ O) _n , n=9-10 | 0.2 | 0.4 | 0.015 |

The topography and phase image of fresh mica, mica aged in crude oil, and those followed by treating with surfactants were prepared at several points of the surface. In each case, images of similar topography and phase images were easily identified. The trend of calculated surface parameters and corresponding phase image profiles were found to be nearly the same for similar images of the case under study.

Results and Discussion

AFM Test. To find the nano-scale wettability changes, the treated and fresh mica surfaces were monitored and topography and phase images were checked to gain the information of surface properties. Phase images show the variations in composition, friction, and other properties according to adhesion force or hardness of the surface. The surface is normally examined by monitoring similarities and contrasts of the image colors, which indicate changes in height and properties of the sample surface, known as topography and phase image, respectively.

The AFM image enables us to gain more information, such as height distribution and roughness parameters, on the basis of a specific area.

Several parameters have to be collected to evaluate and compare surfaces quantitatively, such as S_z , S_a , S_q and S_{ds} , according to eqs 1, 2, 3, and 4, respectively. The summits and valleys are defined as the points that are higher than all eight neighboring points. Note that the points on the edge of the

Table 3. Some Parameters of Mica Surfaces

| substrate | S_z (nm) | S_a (nm) | S_q (nm) | S_{ds} (mm ⁻²) |
|----------------------------------|------------|------------|------------|------------------------------|
| fresh mica | 3.03 | 0.3 | 0.38 | 7×10^{-5} |
| aged mica | 1690 | 255 | 337 | 201900 |
| treated with C ₁₆ TAB | 646 | 64.1 | 110 | 130000 |
| treated with Triton X-100 | 2260 | 312 | 429 | 50800 |

area are not considered.²⁸

$$S_z = \frac{\sum_{i=1}^5 |\text{peak heights}| + \sum_{i=1}^5 |\text{valley depths}|}{5} \quad (1)$$

$$S_a = \iint_a |Z(x, y)| dx dy \quad (2)$$

$$S_q = \sqrt{\iint_a (Z(x, y))^2 dx dy} \quad (3)$$

$$S_{ds} = \frac{\text{number of peaks}}{\text{area}} \quad (4)$$

In Figure 1a-1, the topography and height image of a fresh mica surface is presented. The range of height distributions of the scanned area based on the color variations for untreated mica is lower than 10 nm. The mean roughness, S_a , in Table 3 also shows that the average height distribution of mica is 1.44 nm. A specific path shown by the black arrow in Figure 1a-2 was chosen to make a profile for each image that facilitates the comparison between micro- and nano-scale measurements. The profile of the selected path for the fresh mica surface, in 1D, is shown in Figure 1b.

(28) Danish Micro Engineering A/S (DME). *DualScope/Rasterscope SPM Program*, version 1.6.0; DME: Copenhagen, Denmark, 2010 (www.dme-spm.com).

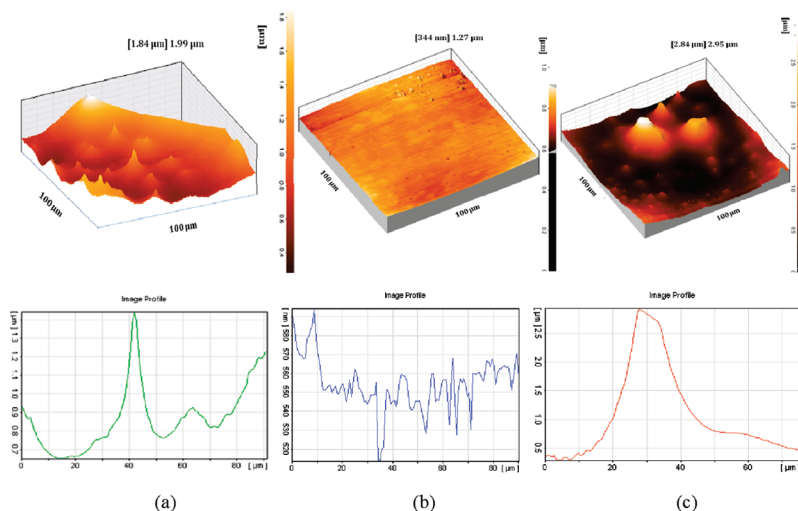


Figure 2. Three-dimensional height images of (a) aged mica, (b) aged mica surface treated with $C_{16}TAB$, and (c) aged mica surface treated with Triton X-100.

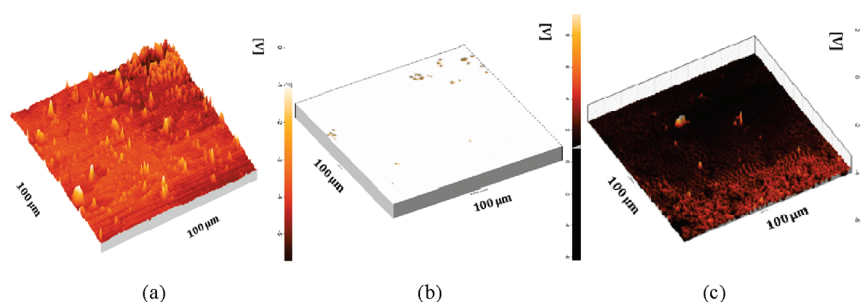


Figure 3. Phase images of (a) aged mica, (b) mica surface treated with $C_{16}TAB$, and (c) mica surface treated with Triton X-100.

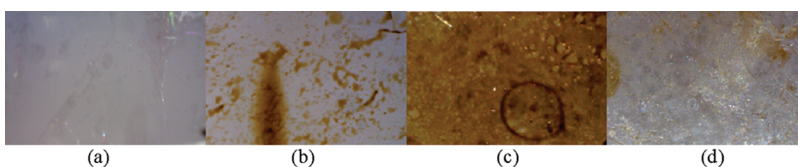


Figure 4. Original images taken by a digital microscope of (a) fresh mica, (b) aged mica, (c) aged mica surface treated with $C_{16}TAB$, and (d) aged mica surface treated with Triton X-100.

The treated samples were prepared on the basis of the mentioned procedure and scanned by AFM using the same mode. The topography and phase images of the aged-mica surface followed by treating with a surfactant were shown in Figures 2 and 3, respectively. The original images of each sample taken by a digital microscope are also shown in panels a–d of Figure 4.

In Figure 2a, the 3D height image of the mica surface aged in crude oil is shown. The topography shows so many peaks and valleys. In comparison to fresh mica (Figure 1a-1), it can be seen that crude oil is adsorbed on the surface as a non-uniform film. The aged surface has the most peak density and non-uniformity, which can be seen in Table 3 as S_{ds} , the number of summits per unit area. Figure 2b shows the same AFM image of the aged mica surface followed by treatment by $C_{16}TAB$. The most important characteristic of this surface is the uniformity of the roughness because of closely spaced valleys and peaks. The mean value of roughness (S_z) shown in Table 3 and the average of the height distributions indicate critical reduction to the nanometer scale when compared to the case of the aged surface with crude oil. By

visual inspection of topography images (Figures 2b and 1a-1), both surfaces seem to be the same with respect to the clarity and roughness distribution. However, the calculated parameters in Table 3 show significant changes, which indicate that a new homogeneous surface is formed.

Figure 2c shows the topography of the mica surface treated with Triton X-100. The surface has fewer peaks and valleys compared to the surface aged in crude oil, which is also evident by the lower value of S_{ds} (Table 3). A comparison of S_z and S_a values (Table 3) demonstrates that the height difference between peaks and valleys is amplified by a factor of 2, while their population is reduced for the surface treated with Triton X-100. On the basis of the topography images (Figure 2) and the surface parameters presented in Table 3 and finally approved by phase images (of the same samples), two different mechanisms for this surface change are proposed. In the first mechanism, Triton X-100 cleans the thin adsorbed oil film and, therefore, amplifies the existing peaks. In the second one, Triton X-100 could be adsorbed on the aged surface, which was primarily recognized as a surface consisting of small and

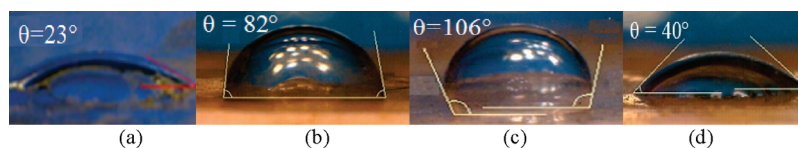


Figure 5. Contact angles of a water drop at kerosene phase on (a) fresh mica, (b) aged mica, (c) soaked mica in $C_{16}TAB$, and (d) soaked mica in Triton X-100.

large peaks,²⁹ reducing the summit density and heterogeneity.

The phase image describes the chemical effects on the aged mica surface, which can be matched with the results obtained from the height of peaks and roughness parameters. The phase image of the surface aged in the crude oil (Figure 3a) is approximately homogeneous, indicating that the oil covers the whole mica surface with different heights, as evident from the topography distributions (see Figure 2a). Shown in Figure 3b, the phase image corresponding to the treated mica surface by $C_{16}TAB$ solution after aging in crude oil verifies the height image of Figure 2b. Therefore, a uniform film of $C_{16}TAB$ is adsorbed. Figure 4c shows that the oil film remained with any obvious change on the mica surface after $C_{16}TAB$ treatment. This can also be verified by comparing the values of roughness to the fresh mica surface image. Figure 2b will be explained in the fractal calculation part in detail. Figure 3c shows phase changes of the surface treated with Triton X-100, and two different substances are seen on the surface. It is important to note that bright points of the phase image are matched with the summits in their height image (compare Figure 3c to Figure 2c). Therefore, the phase image confirms the first mentioned mechanism that Triton X-100 has the ability to clean some parts of the surface, mostly thin film and short summits of the adsorbed oil. This shows that the thick adsorbed layer, which is formed in the shape of high peaks, is not affected by Triton X-100 treatment. This phenomenon may be explained by the fact that summits have stronger and more stable interactions compared to the thin adsorbed films. Figure 4d also visually confirms this mechanism.

Contact Angle Measurements. To support the change in wettability of the surfaces tested by AFM, contact angle measurement of a water droplet in oily phase (kerosene) was conducted for each substrate. The contact angle measured for the fresh mica sample shows that the surface is strongly water-wet, with the water contact angle equal to 23° (Figure 5a). After aging with crude oil, the contact angle was increased to 82° , modifying the surface to almost neutral-wet (Figure 5b). The contact angle of aged mica followed by soaking in $C_{16}TAB$ was increased to 106° (Figure 5c), indicating an oil-wetness condition. The same procedure repeated for the aged mica followed by soaking in Triton X-100 brought about a more water-wetness condition and reduced the contact angle to 40° (Figure 5d). These results in conjunction with the wettability of the surfaces tested by AFM imply that the first mechanism suggested for Triton X-100, cleaning the thin and short peaks of the oil layer, is verified.

Fractal Analysis. The surface fractal dimension has been used in the past to compare the results and to make quantitative analysis from the AFM images.^{29,30} The distribution

Table 4. Fractal Dimension of Treated Mica Surfaces

| type of surfaces | calculated fractal dimension |
|----------------------------|------------------------------|
| fresh mica | 2.8 |
| aged mica (with crude oil) | 2.2 |
| treated with Triton X-100 | 2.1 |
| treated with $C_{16}TAB$ | 2.9 |

of the wetting phase on a surface is affected by the roughness of the surface.^{31–33} Smoothness of an isotropic surface could be characterized by the surface fractal dimension. The surface fractal dimension value is in the range of 2–3, where a smooth surface has a value of 2 and an increasing value of D represents an increasing surface roughness.³⁴

Height data are extracted from the AFM topography image to model the treated mica surfaces and calculate surface fractal dimension. The surface fractal dimensions of different surfaces are shown in Table 4. The height profiles of a line drawn between two points in the AFM image are also shown in Figures 1b and 2.

As seen in Table 4, the surface fractal dimension for fresh mica is equal to 2.8 and the surface fractal dimension for aged mica surface treated with $C_{16}TAB$ is equal to 2.9. On the other hand, the surface fractal dimensions of the surfaces aged in the crude oil and treated with Triton X-100 are calculated to be 2.1 and 2.2, respectively. Although it is known that peeled mica has a smooth surface, the AFM test at very high resolution of a few nanometers shows a rough surface with a fractal dimension of 2.8. In these tests, the main focus is on the variation of fractal dimensions of different surfaces at different conditions instead of their exact values. These results show that the aging of mica in the crude oil followed by treating with Triton X-100 would result in more smooth surfaces because of the ability of this surfactant to remove oil summits.²⁹

Proposed Mechanisms. The wettability alteration mechanism of mica surfaces aged in the crude oil has been studied in the literature.^{20,35–37} Because the pH (7) of used brine corresponds to a higher ξ -potential characteristic of the mica, the negatively charged mica surface thus prepared can adsorb suitably the positive species, e.g., basic compounds. Therefore, the polar compounds with a dipolar interaction and positively charged species with an electrostatic interaction are adsorbed on the active sites of the mica surface effectively. Triton X-100 could be adsorbed as described here by the virtue of its polarizable π electrons.³⁸

(31) Bartell, F. E.; Sheard, J. W. *J. Phys. Chem.* **1953**, *57*, 455–458.

(32) Cassie, A. B. D.; Baxter, S. *Trans. Faraday Soc.* **1944**, *40*, 546–551.

(33) Wenzel, R. W. *Ind. Eng. Chem. Res.* **1936**, *28*, 988–994.

(34) Othman, M. R.; Mustafa, N. N. N.; Ahmad, A. L. *Microporous Mesoporous Mater.* **2006**, *91*, 268–275.

(35) Buckley, J. S.; Takamura, K.; Morrow, N. R. *SPE Form. Eval.* **1989**, 332–340.

(36) Buckley, J. S.; Lord, D. L. *J. Pet. Sci. Eng.* **2003**, *39*, 261–273.

(37) Liu, L.; Buckley, J. S. *J. Pet. Sci. Eng.* **1999**, *24*, 75–83.

(38) Rosen, M. J. *Surfactants and Interfacial Phenomena*; John Wiley and Sons: New York, 1979; pp 40–42.

(29) Sayyad Amin, J.; Ayatollahi, Sh.; Alamdari, A. *Appl. Surf. Sci.* **2009**, *256*, 67–75.

(30) Risovic, D.; Mahovic Poljacek, S.; Furic, K.; Gojo, M. *Appl. Surf. Sci.* **2008**, *255*, 3063–3070.

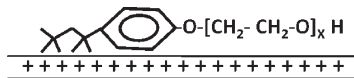


Figure 6. Adsorption of Triton X-100 from aqueous solution via aged mica.

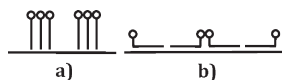


Figure 7. Adsorption of $C_{16}TAB$ via (a) hydrophobic interaction and (b) dispersion forces on aged mica.

Because Triton X-100 (adsorbate) contains electron-rich aromatic nuclei and the aged mica has positive sites, the attraction interaction between them is enhanced, leading to an effective adsorption, as demonstrated schematically in Figure 6.

On the other hand, for $C_{16}TAB$, an efficient hydrophobic interaction can occur as shown in Figure 7a, while the positive headgroup is repelled by the positive surface. Because the adsorbed oil undergoes a competition in a hydrophobic interaction with $C_{16}TAB$, the more strongly adsorbed oil does not provide much chance for wettability alteration, which is normally expected by the virtue of the $C_{16}TAB$ surfactant.³⁸ The adsorption could also occur by London–van der Waals dispersion forces acting between adsorbent and adsorbate molecules (Figure 7b).

Conclusions

The AFM results confirmed that the wettability alteration process of the surfactant-treated mica surfaces aged initially in the crude oil using Triton X-100 is more efficient than using $C_{16}TAB$.

Contact angle measurements show that Triton X-100 could change the wettability of the mica surface aged in crude oil to water-wet but $C_{16}TAB$ changes it to the more oil-wet condition.

Two different mechanisms proposed here are surface cleaning and surfactant adsorption for Triton X-100 and $C_{16}TAB$, respectively.

The results of surface fractal dimension analysis indicate that the wettability alteration could be monitored directly through the surface roughness inspection.

Acknowledgment. The authors thank the Research and Technology Directorate of NIOC for supporting this project under Project 81-86014. They are also greatly thankful to Ehsan Nikoee from the Department of Civil Engineering, Shiraz University, for his valuable comments and help in performing fractal analyses on the AFM images.

Nomenclature

- S_z = height of 10 points
- S_a = mean roughness
- S_q = root-mean-square deviation
- S_{ds} = density of summits
- D = surface fractal dimension